



ARL-TR-7416 • SEP 2015



Numerical Simulation of Ballistic Impact of Layered Aluminum Nitride Ceramic

by JD Clayton

Approved for public release; distribution unlimited.

NOTICES

Disclaimers

The findings in this report are not to be construed as an official Department of the Army position unless so designated by other authorized documents.

Citation of manufacturer's or trade names does not constitute an official endorsement or approval of the use thereof.

Destroy this report when it is no longer needed. Do not return it to the originator.



Numerical Simulation of Ballistic Impact of Layered Aluminum Nitride Ceramic

by JD Clayton

Weapons and Materials Research Directorate, ARL

REPORT DOCUMENTATION PAGE			Form Approved OMB No. 0704-0188		
Public reporting burden for this collection of information is estimated to average 1 hour per response, including the time for reviewing instructions, searching existing data sources, gathering and maintaining the data needed, and completing and reviewing the collection information. Send comments regarding this burden estimate or any other aspect of this collection of information, including suggestions for reducing the burden, to Department of Defense, Washington Headquarters Services, Directorate for Information Operations and Reports (0704-0188), 1215 Jefferson Davis Highway, Suite 1204, Arlington, VA 22202-4302. Respondents should be aware that notwithstanding any other provision of law, no person shall be subject to any penalty for failing to comply with a collection of information if it does not display a currently valid OMB control number. PLEASE DO NOT RETURN YOUR FORM TO THE ABOVE ADDRESS.					
1. REPORT DATE (DD-MM-YYYY) September 2015		2. REPORT TYPE Final		3. DATES COVERED (From - To) January 2015–April 2015	
4. TITLE AND SUBTITLE Numerical Simulation of Ballistic Impact of Layered Aluminum Nitride Ceramic			5a. CONTRACT NUMBER		
			5b. GRANT NUMBER		
			5c. PROGRAM ELEMENT NUMBER		
6. AUTHOR(S) JD Clayton			5d. PROJECT NUMBER FPEC-99		
			5e. TASK NUMBER		
			5f. WORK UNIT NUMBER		
7. PERFORMING ORGANIZATION NAME(S) AND ADDRESS(ES) US Army Research Laboratory ATTN: RDRL-WMP-C Aberdeen Proving Ground, MD 21005-5066			8. PERFORMING ORGANIZATION REPORT NUMBER ARL-TR-7416		
9. SPONSORING/MONITORING AGENCY NAME(S) AND ADDRESS(ES)			10. SPONSOR/MONITOR'S ACRONYM(S)		
			11. SPONSOR/MONITOR'S REPORT NUMBER(S)		
12. DISTRIBUTION/AVAILABILITY STATEMENT Approved for public release; distribution unlimited					
13. SUPPLEMENTARY NOTES					
14. ABSTRACT Numerical simulations of ballistic impact and penetration by tungsten rods into targets consisting of layers of aluminum nitride ceramic tile(s), polymer laminae, and aluminum backing are conducted over a range of impact velocities on the order of 1.0 to 1.2 km/s. Results for ballistic efficiency are compared with experimental data from the literature. Predicted residual penetration depths tend to exceed corresponding experimental values, though simulations and experiments both demonstrate a trend of decreasing efficiency with increasing impact velocity. Closest agreement is obtained when polymer interfaces are not explicitly represented, suggesting the current model representation of such interfaces is overly compliant. Results emphasize the importance of proper resolution of geometry and constitutive properties of thin layers and interfaces between components for accurate numerical evaluation of performance of modern composite protection systems.					
15. SUBJECT TERMS terminal ballistics, armor, ceramics, metals, modeling and simulation					
16. SECURITY CLASSIFICATION OF:			17. LIMITATION OF ABSTRACT UU	18. NUMBER OF PAGES 18	19a. NAME OF RESPONSIBLE PERSON JD Clayton
a. REPORT Unclassified	b. ABSTRACT Unclassified	c. THIS PAGE Unclassified			19b. TELEPHONE NUMBER (include area code) 410-278-6146

Contents

List of Figures	iv
List of Tables	iv
1. Introduction	1
2. Approach	2
3. Results	4
4. Conclusions	8
5. References	10
Distribution List	12

List of Figures

Fig. 1	Ballistic impact problem: a) projectile and target (3 tiles) and b) finite element mesh	1
Fig. 2	Penetration into bare aluminum backing material: a) depth vs. impact velocity for simulation and experiment and b) simulation result at impact velocity of 1,030 m/s	5
Fig. 3	Penetration simulations into ceramic-metal targets: a) one tile, tied bonding, impact velocity 1,030 m/s, b) 3 tiles, free bonding, with polymer, impact velocity 1,100 m/s, and c) 6 tiles, free bonding, without polymer, impact velocity 1,160 m/s.....	6
Fig. 4	Ballistic efficiency vs. impact velocity for ceramic-metal targets from simulations and experiments: a) 1 tile, b) 3 tiles, and c) 6 tiles.....	7
Fig. 5	Residual penetrator velocity vs. impact velocity from simulations: a) 3 tiles and b) 6 tiles.....	7

List of Tables

Table 1	Materials and constitutive models	2
Table 2	Numerical simulations	4

1. Introduction

Modern protection systems often consist of layers of ceramic, metallic, and/or polymer-based components. Interfaces between layers may strongly influence performance of such systems under ballistic impact. However, the importance of interfacial characteristics (e.g., interface thickness, material type, and bonding strength) is not fully understood in many cases. Furthermore, the accuracy of available computational tools to assess such effects has heretofore not been quantified. The purpose of this study is assessment of one computational tool—with typical/default user options enabled—for modeling ballistic impact and penetration of a layered target consisting of one or more ceramic tiles backed by a thick metallic plate, with layers of polymer between the tiles in some cases. The focus is evaluation of the fidelity of existing models and numerical methods; modification of material models or calibration of user-defined parameters to best match experimental ballistic results is beyond the scope of the present study.

Specifically, the penetrator-target configuration simulated in this work duplicates that examined in experiments of Yadav and Ravichandran.¹ As shown in Fig. 1a, a WHA (tungsten heavy alloy) penetrator, cylindrical in shape with flat nose, impacts a target at velocity V ranging from approximately 1,000 to 1,200 m/s at null obliquity. The respective length L and diameter D of the penetrator are 50.6 mm and 8.43 mm ($L/D = 6$). The target consists of 1, 3, or 6 tiles of aluminum nitride (AlN), a polycrystalline ceramic. The total thickness of the tile(s) is 38.1 mm in all cases. A thin polyurethane laminate separates neighboring tiles in the experiments when the target contains multiple tiles.

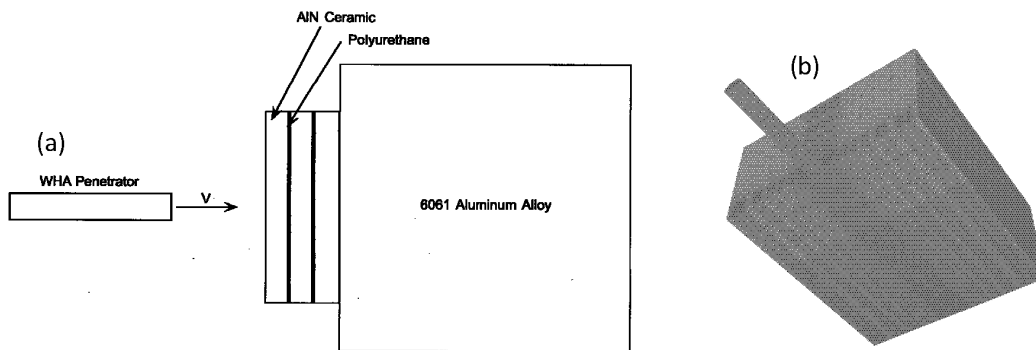


Fig. 1 Ballistic impact problem: a) projectile and target (3 tiles) and b) finite element mesh

Ballistic performance of the ceramic-polymer system (or a single tile in some cases) is quantified by residual penetration depth into a 6061-T6 aluminum (Al) backing block of thickness 76.2 mm, which was sufficient to fully stop the penetrator in all

reported experiments.¹ The main result reported from the experimental study was that ballistic efficiency was highest (best) for 3 tiles, each of thickness 12.7 mm; intermediate for a single tile of thickness 38.1 mm; and lowest (worst) for 6 tiles, each of thickness 6.35 mm. Lateral tile dimensions were 101.6 × 101.6 mm. It was speculated that soft polymer layers in the 3-tile configuration enabled dispersion of the initial, primary compressive shock wave that caused more severe damage in the single tile configuration. On the other hand, bending and tensile failure modes were posited to strongly and negatively influence penetration resistance of the 6-tile configuration, more than offsetting any benefits obtained by dispersion or attenuation of the initial compressive shock attributed to the presence of compliant polymer layers and weak interfaces.

The computational tool implemented in this study is the EPIC (Elastic Plastic Impact Calculation) finite element code² (2013 release). This code was chosen for 2 primary reasons: 1) its existing library of material models is extensive and was thought sufficient for representation of behaviors of each component (ceramic, polymer, and metals as listed in Table 1) and 2) its graphical user interface permits rapid generation of finite element meshes for ballistic penetration simulations of layered targets, as shown for example in Fig. 1b.

Table 1 Materials and constitutive models

Component	Material	EPIC Material Number	Reference
Ceramic tile(s)	Aluminum nitride (AlN)	163	a
Polymer layers	Polyurethane foam	18	b
Backing metal	Aluminum 6061-T6 (Al)	23	c
Projectile	Tungsten heavy alloy (WHA)	157	c

^aJohnson GR, Holmquist TJ, Beissel SR. Response of aluminum nitride (including a phase change) to large strains, high strain rates, and high pressures. *Journal of Applied Physics*. 2003;94:1639–1646.

^bMatuska DA, Durrett RE, Osborn JJ. Hull user guide for three-dimensional linking with EPIC-3. Aberdeen Proving Ground (MD): Army Ballistic Research Laboratory (US); 1982. Technical Report No.: ARBRL-CR-00484.

^cJohnson GR, Cook WH. A constitutive model and data for metals subjected to large strains, high strain rates and high temperatures. *Proceedings of the 7th International Symposium on Ballistics*; 1983 Apr 19–21; The Hague, Netherlands. p. 541–547.

2. Approach

Tetrahedral finite element meshes were generated using the EPIC preprocessor with the default fine mesh setting and expanded grid, the latter feature leading to progressive mesh coarsening with increasing distance from the penetration zone. This mesh density was found sufficient to yield a mesh size-independent result for residual penetration depth; in fact, an even coarser medium mesh setting was usually sufficient but not used. As shown in Table 2, cases with and without

polymer layers were simulated. In the former, the thickness of polymer layers was restricted by constraints imposed by the mesh generator to a minimum value of 1.054 mm, about 4 times thicker than the value of 0.254 mm tested experimentally.¹ Resolution of the latter very small thickness would require extremely small elements, which in turn would drastically increase computational cost through time step reductions imposed by the Courant condition.

Table 2 Numerical simulations

Number of Tiles × Thickness (mm)	Bonding	Polymer	V (m/s)	P/L	η	V_R/V
1 × 38.1	Free	No	1,030	0.502	0.842	0
			1,100	0.757	0.775	0
			1,160	1.038	0.718	0
	Tied	No	1,030	0.136	0.957	0
			1,100	0.194	0.942	0
			1,160	0.617	0.828	0
3 × 12.7	Free	No	1,030	1.182	0.628	0
			1,100	1.377	0.591	0
			1,160	...	0	0.233
	Free	Yes	1,030	1.532	0.518	0
			1,100	...	0	0.183
			1,160	...	0	0.357
	Tied	Yes	1,030	...	0	0.115
			1,100	...	0	0.233
			1,160	...	0	0.304
6 × 6.35	Free	No	1,030	1.026	0.677	0
			1,100	1.334	0.603	0
			1,160	...	0	0.219
	Free	Yes	1,030	...	0	0.275
			1,100	...	0	0.352
			1,160	...	0	0.388
	Tied	Yes	1,030	...	0	0.301
			1,100	...	0	0.355
			1,160	...	0	0.417

Material models were selected from library options that best matched those of the experiments; details can be found in Table 1. A notable discrepancy is that the density of the polyurethane polymer material used in experiments is somewhat larger (a factor of 3.8) than the most dense polyurethane foam of the available constitutive models. Default options for element failure were imposed in all simulations: elements were eroded³ when scalar effective strains exceeded a value of 1.5. Nodal masses were conserved upon element erosion, but strength and pressure were zeroed for failed/eroded elements. Frictionless contact between projectile and target was imposed. Interfaces were assigned 1 of 2 conditions: 1) tied bonding, corresponding to shared nodes and perfect coherence, or 2) free contact, corresponding to duplicate nodes with interacting frictionless surfaces. In

some simulations involving multiple tiles, the polymer layers were excluded. The very thin coating of epoxy used to glue the rearmost tile to the backing block in experiments was not modeled explicitly. Far-field boundary conditions corresponded to free surfaces (i.e., the targets were unconfined as in the experiments), though effects of interaction with the mounting apparatus were necessarily excluded in the simulations.

Prior to simulations of the ceramic-polymer-metallic targets, simulations of penetration of the bare backing metal were conducted, similar to those reported in experiments.¹ The thickness of the bare metal target was not reported from the experimental study; a value of $6L$ was used in the simulations, ensuring independence of residual penetration depth P_0 from target thickness. A simulation time of 1.0 ms was sufficient for cessation of relative motion of the projectile to that of the target. Impact velocities of 1,030; 1,100; and 1,160 m/s were considered.

Next, numerical simulations of the layered targets were conducted, for the same 3 impact velocities, as listed in Table 2. Ballistic efficiency η of the ceramic-polymer targets is defined as¹

$$\eta = 1 - P/P_0 = 1 - (P/L)/(P_0/L), \quad (1)$$

where P is the residual penetration depth into the aluminum backing behind the interface between the backing and rearmost AlN tile and P_0 is the residual penetration depth into the bare backing at the same impact velocity. When the projectile completely penetrated the backing metal thickness of 76.2 mm, a value of 0 was assigned to η . In such cases, the residual velocity V_R of the penetrator at a time of 1.0 ms was recorded (Table 2).

Simulations were executed in parallel mode on 16 processors using the available 2013 version of the EPIC code on the Spirit cluster at the US Air Force Research Laboratory. Wall clock execution times were always less than 24 h.

3. Results

Predictions are compared with experiments for the bare backing metal (Al) in Fig. 2a, wherein a linear fit to the data was sufficient to fit results for the 3 impact velocities considered in each case:

$$P_0/L = a_0 + a_1 V, \quad (2)$$

with values of dimensionless constant a_0 and constant a_1 (s/m) shown in Fig. 2a. Shown in Fig. 2b is the residual penetration at 1.0 ms; notice that the damaged zone exceeds the penetration depth of the partially eroded projectile in this case.

Predicted penetration depths significantly exceed experimental values. Reasons for the differences in results cannot be isolated in the present set of simulations, but possibilities include the following: the WHA material may be weaker than that depicted by the model, or the Al material may be stronger than that depicted by the model; the erosion criterion invoked in simulations may be too liberal for the Al or too strict for the WHA; omission of friction and commensurate wear between target and eroding projectile may result in larger penetration depths than observed in experiments; and/or far-field boundary conditions may artificially affect depth of penetration results at later simulation times.

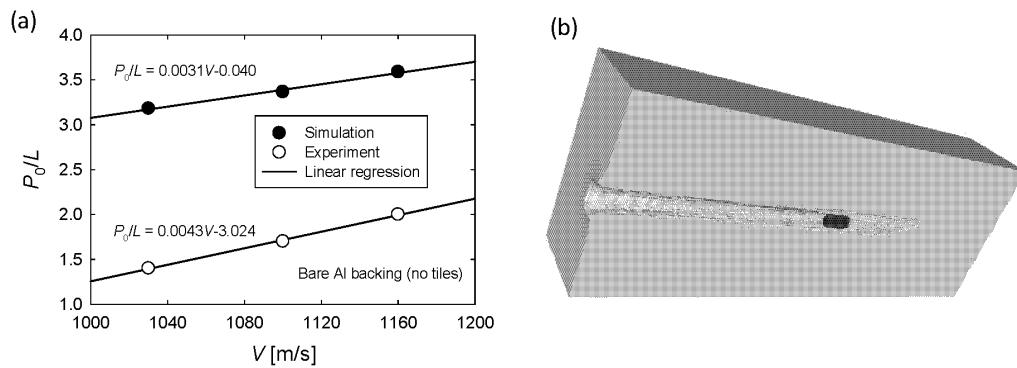


Fig. 2 Penetration into bare aluminum backing material: a) depth vs. impact velocity for simulation and experiment¹ and b) simulation result at impact velocity of 1,030 m/s

Representative results from various target configurations and impact velocities are illustrated in Fig. 3, all corresponding to a solution time of 1 ms. Specifically, in Fig. 3a the penetrator barely defeats the single ceramic tile and resides just inside the metal backing plate ($P/L = 0.136$ in Table 2). In Fig. 3b, the entire target—including 3 ceramic tiles, 2 layers of polymer, and metal backing plate—has been perforated by the projectile, and all layers of polymer laminate have been highly eroded. The latter result agrees qualitatively with experimental observation of severe damage in polymer layers of recovered targets.¹ In Fig. 3c, the initially unbonded 6 ceramic tiles have been shattered by the projectile, which remains lodged at the back free surface of the aluminum backing.

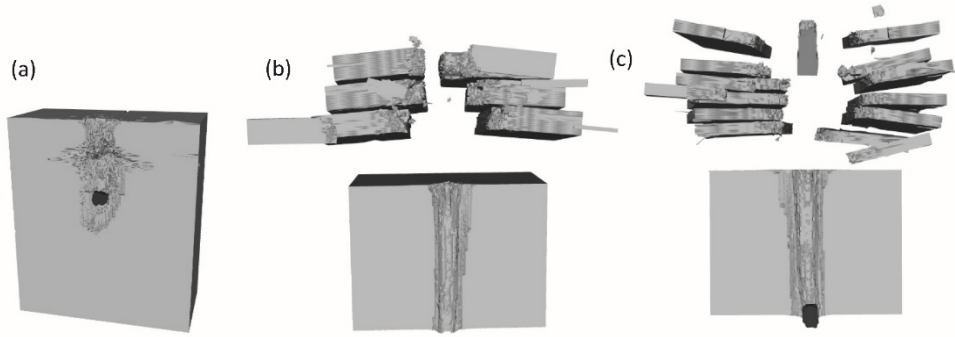


Fig. 3 Penetration simulations into ceramic-metal targets: a) one tile, tied bonding, impact velocity 1,030 m/s, b) 3 tiles, free bonding, with polymer, impact velocity 1,100 m/s, and c) 6 tiles, free bonding, without polymer, impact velocity 1,160 m/s

Ballistic efficiencies from simulations and experiments are compared in Fig. 4. Note that overlapping data points in Fig. 4 (e.g., those when $\eta = 0$ in many instances) can be discerned by examining corresponding numerical values shown in Table 2. In Fig. 4a, simulation results for η for a single ceramic tile exceed those from experiments when the ceramic is perfectly bonded (tied) to the backing plate, while agreement with experiment is closer for free contact between ceramic and backing. For results of the 3-tile configuration shown in Fig. 4b, experimental values of η exceed simulation predictions regardless of bonding or inclusion of polymer layers, though closest agreement is obtained when polymer layers are omitted in the simulations. In Fig. 4c, the same conclusion is drawn for the 6-tile configuration (i.e., closest agreement is obtained when the polymer layers are not explicitly represented in the calculations). The simulations do tend to reflect the experimentally observed trend of decreasing efficiency with increasing impact velocity. When ranked via decreasing ballistic penetration resistance, experimental results suggest an ordering of 3, 1, then 6 tiles, while simulation results suggest an ordering of 1, 3, and then 6 tiles.

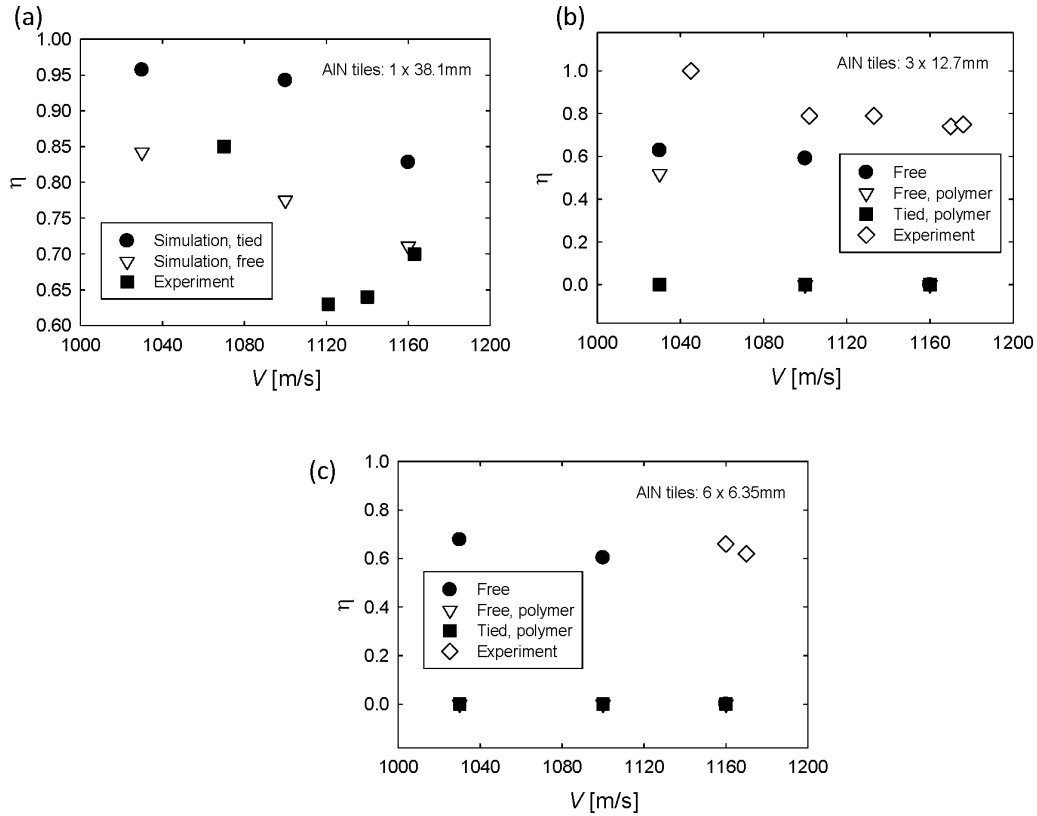


Fig. 4 Ballistic efficiency vs. impact velocity for ceramic-metal targets from simulations and experiments: a) 1 tile, b) 3 tiles, and c) 6 tiles

Residual velocities from simulations at 1.0 ms for 3- and 6-tile target configurations are shown in Fig. 5a and Fig. 5b, respectively. Recall that complete perforation did not occur in any reported experiments.¹ Residual velocities are similar for free interfaces and for tied bonding with polymer, confirming failure and commensurate erosion of the polymer layers and consistent with efficiency results shown in Fig. 4.

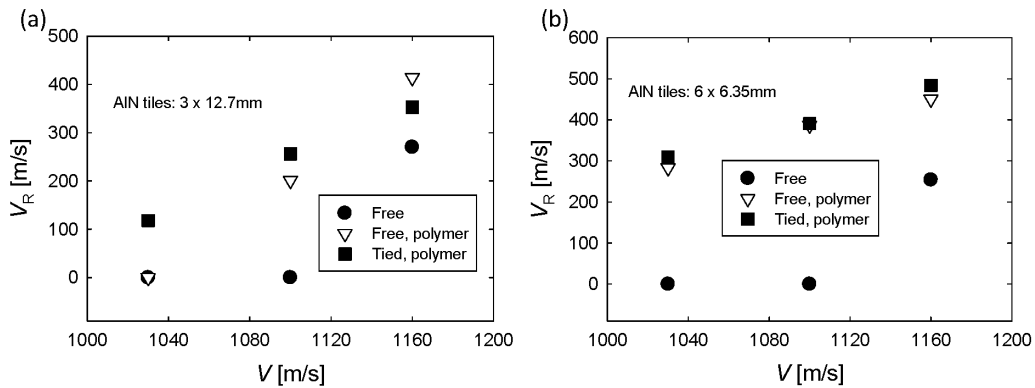


Fig. 5 Residual penetrator velocity vs. impact velocity from simulations: a) 3 tiles and b) 6 tiles

Simulation results suggest that incorporation of compliant polymer layers promotes bending modes and tensile fracture in the ceramic layers, leading to decreased ballistic efficiency relative to simulations wherein polymer is omitted. Furthermore, increasing the number of tiles, while decreasing the individual tile thickness, exacerbates this weakness of the target, especially when more polymer layers are included with increasing number of tiles.

As noted in the context of penetration results for the bare backing metal, the source of discrepancy between model and experiment could not be isolated, but several possibilities can be suggested. Uncertainties in material properties and erosion criteria, omission of contact friction, and possible artifacts of far-field boundary conditions may adversely affect accuracy or precision of results. Another likely source of model discrepancy is the thicker, more compliant polymer representation than that tested experimentally, which would tend to promote target defeat for reasons explained above.

In summary, results in Table 2, Fig. 4, and Fig. 5 demonstrate how resolution of geometry and behavior of thin interfaces between layers of stiff material in armor systems strongly affects predicted ballistic efficiency. It follows that representation of interfaces should be carefully considered by the numerical analyst when constructing finite element or finite difference models for performance evaluations of such systems. Concurrent experiments and validation simulations on systems of lower complexity are recommended for future work, such that sources of discrepancy between model and experiment can be more precisely identified. Cohesive zone representations of interfacial separation⁴ offer the potential for more realistic modeling of interfacial physics than the fully bonded or free surface interactions prescribed herein among layers. Constitutive models with a more rigorous basis in finite deformation kinematics⁵ and thermodynamics⁶ may enable improvements in descriptions of the bulk behavior of metals^{4,7-9} and ceramics^{10,11}, albeit at increased model complexity and computational expense. Phase field models¹² of structural transformations (e.g., for phase transitions and fracture in AlN) may also offer improvement over usual continuum mechanical treatments available in simulation codes such as EPIC.

4. Conclusions

Numerical simulations of ballistic impact and penetration of targets consisting of layers of aluminum nitride ceramic tile(s), polymer laminae, and aluminum backing have been conducted over a range of impact velocities on the order of 1.0 to 1.2 km/s. Results for ballistic efficiency have been compared with experimental data. Predicted residual penetration depths tended to exceed corresponding

experimental values, though simulations and experiments both demonstrated a trend of decreasing efficiency with increasing impact velocity. Closest agreement was obtained when polymer interfaces of small but finite thickness were not explicitly resolved, suggesting the model representation of such interfaces is overly compliant. Results emphasize the importance of proper resolution of geometry and constitutive properties of thin layers and interfaces in numerical evaluation of performance of modern composite protection systems.

5. References

1. Yadav S, Ravichandran G. Penetration resistance of laminated ceramic/polymer structures. *International Journal of Impact Engineering*. 2003;28:557–574.
2. Johnson GR, Stryk RA, Holmquist TJ, Beissel SR. Numerical algorithms in a Lagrangian hydrocode. Eglin Air Force Base (FL): Wright Laboratory; 1997. Technical Report WL-TR-1997-7039.
3. Johnson GR, Stryk RA. Eroding interface and improved tetrahedral element algorithms for high velocity impact calculations in three dimensions. *International Journal of Impact Engineering*. 1997;5:411–421.
4. Clayton JD. Dynamic plasticity and fracture in high density polycrystals: constitutive modeling and numerical simulation. *Journal of the Mechanics and Physics of Solids*. 2005;53:261–301.
5. Clayton JD. *Differential geometry and kinematics of continua*. Singapore: World Scientific Publishing Company; 2014.
6. Clayton JD. *Nonlinear mechanics of crystals*. Dordrecht (The Netherlands): Springer; 2011.
7. Clayton JD, McDowell DL. A multiscale multiplicative decomposition for elastoplasticity of polycrystals. *International Journal of Plasticity*. 2003;19:1401–1444.
8. Clayton JD. Modeling effects of crystalline microstructure, energy storage mechanisms, and residual volume changes on penetration resistance of precipitate-hardened aluminum alloys. *Composites B: Engineering*. 2009;40:443–450.
9. Clayton JD. Two-scale modeling of effects of microstructure and thermomechanical properties on the dynamic performance of an aluminum alloy. *International Journal of Materials and Structural Integrity*. 2010;4:116–140.
10. Clayton JD. A continuum description of nonlinear elasticity, slip and twinning, with application to sapphire. *Proceedings of the Royal Society A*, 2009;465:307–334.

11. Clayton JD. Finite strain analysis of shock compression of brittle solids applied to titanium diboride. *International Journal of Impact Engineering*. 2014;73:56–65.
12. Clayton JD, Knap J. A phase field model of deformation twinning: nonlinear theory and numerical simulations. *Physica D*. 2011;240:841–858.

1 DEFENSE TECHNICAL
(PDF) INFORMATION CTR
DTIC OCA

2 DIRECTOR
(PDF) US ARMY RESEARCH LAB
RDRL CIO LL
IMAL HRA MAIL & RECORDS
MGMT

1 GOVT PRINTG OFC
(PDF) A MALHOTRA

9 DIR USARL
(PDF) RDRL WMP
S SCHOENFELD
RDRL WMP C
R BECKER
S BILYK
T BJERKE
J CLAYTON
R LEAVY
J LLOYD
A TONGE
RDRL WMP D
R DONEY